Inorganic Nanotubes

DOI: 10.1002/anie.200502665

Porous Silicon and Alumina as Chemically Reactive Templates for the Synthesis of Tubes and Wires of SnSe, Sn, and SnO_2**

*Lili Zhao, Maekele Yosef, Martin Steinhart, Petra Göring, Herbert Hofmeister, Ulrich Gösele, and Sabine Schlecht**

Highly ordered porous templates such as alumina membranes[1] and macroporous silicon[2] are valuable and versatile tools for the fabrication of arrays of one-dimensional nanostructures with high aspect ratios and narrow diameter distributions.[3] With templates of macroporous silicon and porous alumina, pore diameters from 25 nm up to 1000 nm are accessible. Here, we report on a new synthetic approach where these templates are not simply inert shape-defining molds but also chemical reagents for the oxidation or reduction of tin(II) selenide. For a given template system, the reduction or oxidation can be initiated easily by increasing the temperature to $\approx 650\,^{\circ}C$. Starting from tin(II) selenide nanotubes with tin in a medium oxidation state, single-crystalline nanotubes of elemental tin were produced in a high-temperature reaction with the macroporous silicon template as a reducing environment. In an analogous manner single-crystalline nanowires of tin(IV) oxide (SnO_2) were obtained using the high-temperature oxidizing proper-

[*] Dr. M. Yosef, Prof. Dr. S. Schlecht
Institut für Chemie und Biochemie
Freie Universität Berlin
Fabeckstrasse 34–36, 14195 Berlin (Germany)
Fax: (+49) 30-838-53310
E-mail: schlecht@chemie.uni-marburg.de
L. Zhao, Dr. M. Steinhart, Dr. P. Göring, H. Hofmeister, Prof. Dr. U. Gösele
Max-Planck-Institut für Mikrostrukturphysik
Halle (Germany)

[**] This research was supported financially by the Deutsche Forschungsgemeinschaft (SPP1165 "Nanowires and Nanotubes", STE1127/2-1 and SCHL529/2-1) and the Fonds der Chemischen Industrie. We thank T. Geppert, K. Sklarek, and S. Grimm for preparing the templates.

ties of the pore walls of alumina templates etched with sulfuric acid.

It is known that SnSe forms as the primary thermolytic product of the precursor $Sn(SePh)_4$[4] at temperatures above 300 °C. SnSe is a narrow-band-gap semiconductor with an optical band gap of ≈ 1 eV. In particular, nanoscale thin films of the tin(II) chalcogenides SnS and SnSe are promising materials for photoelectric conversion.[5,6] Polycrystalline films of SnSe can be used in energy-conversion devices[6] and in memory switching.[7] Ordered structures of tin nanotubes can be used for the preparation of nanostructures of catalytically active binary intermetallics such as Pt–Sn[8] and Au–Sn.[9] Tin nanowires also exhibit superconducting properties.[10] Nanoribbons, nanowires, and nanoboxes[11] of tin(IV) oxide were produced by template-assisted routes or by addition of surface-capping additives and showed excellent sensing properties. The different types of templates we used for the preparation of nanowires and nanotubes of SnSe, Sn, and SnO_2 are listed in Table 1.

Table 1: Redox properties of different template types at elevated temperatures.

Template type	Pore diameter	Redox properties
alumina (etched with sulfuric acid)	25 nm, 30 nm	oxidizing
alumina (etched with phosphoric acid)	180 nm, 400 nm	mostly inert
silicon	1000 nm	reducing

Self-ordered porous alumina is currently accessible with pore diameters ranging from 25 nm to 400 nm and pore depths up to 100 μm. The pore walls are amorphous and also contain tetrahedrally coordinated aluminum atoms, defects, and electrolyte anions.[12,13] Commonly used electrolytes are sulfuric acid,[1c] yielding pores with a diameter of 25 nm, and phosphoric acid,[1d] yielding pores with a diameter of 180 nm. The latter pores can be widened to 400 nm by an isotropic wet-etching step. The properties of the pore walls depend to a great extent on the electrolyte, and the more acidic medium of sulfuric acid together with a higher defect concentration in thin pore walls should enhance the reactivity of the templates with small pore diameters (Table 1). Macroporous silicon templates cover the diameter range from 370 nm up to few microns. Their pore depths are limited only by the thickness of the wafers used as substrates and can reach several hundreds of microns,[2] thus leading to excellent aspect ratios of the pores.

Independent of the produced target material, solid wires formed in narrow pores with diameters of 25 nm, whereas tubes were obtained when pores with diameters of 180, 400, or 1000 nm were used. All products resulting from a thermolysis at 350 °C showed a granular, polycrystalline morphology. When higher temperatures of 600 °C to 650 °C were applied, the formation of single-crystalline wires and tubes was achieved. The transition from wires to tubular structures depending on the pore diameter of the templates also occurs in the case of the template-assisted thermolysis of hydrogen tetrachloroaurate leading to gold nanostructures.[3i]

In the wetting procedure applied here, the single-source precursor $Sn(SePh)_4$ is infiltrated into the pores. In a low-temperature thermolysis at about 350 °C SnSe forms as the initial thermolytic product and no chemical reaction involving the template and the precursor or the template and the produced SnSe takes place. Nanowires consisting of orthorhombic SnSe (space group *Pbnm*)[14] with a diameter of 25 nm, corresponding to the diameter of the template pores, were obtained when the wetted samples were annealed at 350 °C for 36 h. A transmission electron microscopic (TEM) image of a bundle of released polycrystalline SnSe nanowires is shown in Figure 1 a, and the corresponding selected area electron diffraction pattern (SAED) is shown in Figure 1 b. An X-ray diffraction pattern of the SnSe nanowires, which indicates the formation of single-phase SnSe, is represented in Figure 1 c.

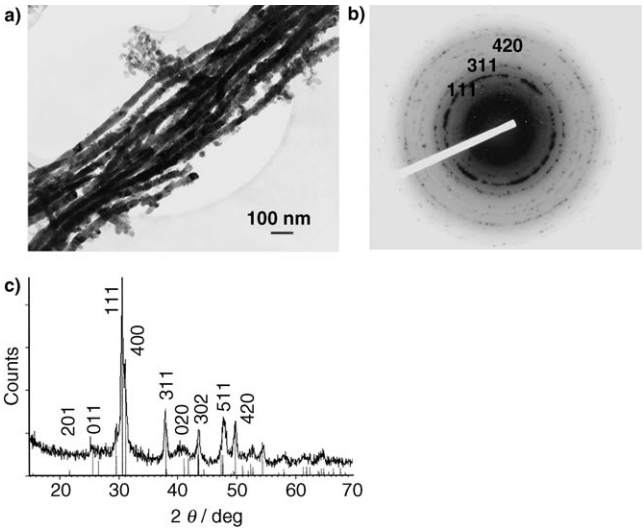

Figure 1. a) TEM image of a bundle of released SnSe nanowires with a diameter of 25 nm; b) electron diffraction pattern of a bundle of SnSe nanowires; c) XRD pattern of SnSe nanowires in the template (reflections are calculated as a line pattern and indexed according to JCPDS card no. 88-0287).

Nanotubes of SnSe with polycrystalline walls formed when porous alumina with a pore diameter of 180 nm was used as a template. The scanning electron micrographic (SEM) images in Figure 2 a and b show an overview and a magnified image of an array of aligned SnSe nanotubes released from the template. In Figure 2 b it can be seen that the nanotubes have terminating caps at their ends, resulting from the bottom dimple of the template pores. This detail nicely shows that the pores were filled in their full depth and that the excellent aspect ratio of the pores can be transferred quantitatively to the one-dimensional nanostructures. The grain structure of the tube walls is apparent in Figure 2 c, where an individual polycrystalline SnSe tube released from a template with a pore diameter of 400 nm is depicted. The crystallites have diameters on the order of 10–20 nm. The thickness of the tube walls is also in the range of 20 nm. The SAED pattern depicted in Figure 2 d shows the characteristics

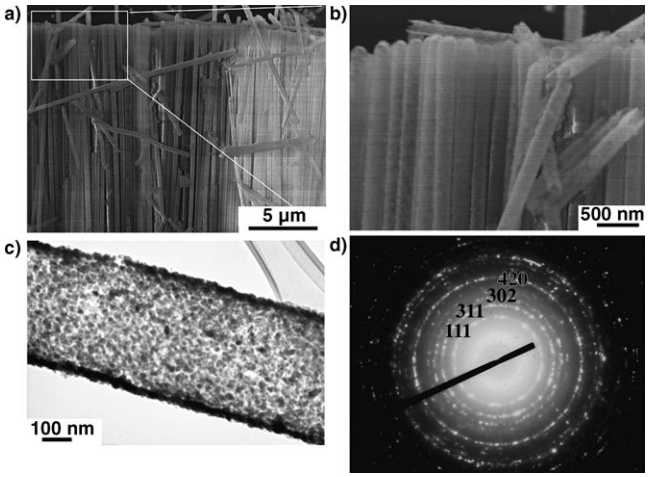

Figure 2. SEM images of an ordered array of SnSe nanotubes with a diameter of 180 nm: a) overview; b) magnified image showing granular wall morphology and terminating caps; c) TEM image of a single SnSe nanotube with a diameter of 400 nm and polycrystalline walls; d) electron diffraction pattern of the tube section seen in (c).

of polycrystalline tubes of single-phase orthorhombic SnSe (space group *Pbnm*).

The intermediate oxidation state of Sn^{II} in SnSe offers the opportunity of either a reduction or an oxidation of the SnSe nanostructures by appropriate pore walls with reducing or oxidizing properties. Such selective redox chemistry within the pores requires that the pore walls of the alumina templates have sufficient oxidizing power and that the pores of the macroporous silicon have good reducing ability, as these two template materials are the most readily accessible ones with complementary redox properties.

To model the redox chemistry of $Sn(SePh)_4$ and SnSe with macroporous silicon and with the pore walls of porous alumina, the two tin compounds were reacted with commercial silicon powder under different conditions (Table 2), and

Table 2: Overview of reactions of $Sn(SePh)_4$ and SnSe with silicon (reaction time: 15 h).

Tin compound	Silicon source	Reaction temperature	Product
$Sn(SePh)_4$	Si template	650 °C	Sn
$Sn(SePh)_4$	Si powder	500 or 600 °C	SnSe
$Sn(SePh)_4$	Si powder	650 °C	Sn
SnSe (nanopart.)	Si powder	650 °C	Sn
SnSe (microcryst.)	Si powder	650 °C	SnSe, very little Sn

the molecular precursor $Sn(SePh)_4$ was heated in boiling wet diethylene glycol solvent, a system with hydroxy groups and a small water content just like the amorphous wall structure of the pores in ordered alumina membranes.[12,13,15] Under these conditions $Sn(SePh)_4$ did not thermolyze into SnSe but was converted into nanoparticles of SnO_2 with a diameter of about 10 nm, as could be shown by X-ray powder diffraction. In a series of experiments with silicon powder the formation of elemental tin was observed at reaction temperatures higher than 600 °C (Table 2). The reduction can be performed as a quantitative conversion either starting directly from molecular $Sn(SePh)_4$ or from independently produced nanoparticles of SnSe with a particle size of ≈50 nm. In both reactions elemental tin was formed under the reaction conditions and crystallized from its liquid state under cooling. Owing to the large surface area of the pore walls of macroporous silicon templates and a relevant number of defects and distortions that form in the structure of the pore walls of macroporous silicon during annealing,[3h] the reaction of $Sn(SePh)_4$ with the template pores should be even more effective than its reaction with microcrystalline silicon powder. Accordingly, single-crystalline microtubes consisting of elemental Sn with a diameter of 1 μm were obtained by infiltrating macroporous silicon molds with $Sn(SePh)_4$, annealing the wetted templates at temperatures in the range of 600–650 °C for 5 h, and subsequently cooling the samples to room temperature at a rate of 2 K min^{-1}. Figure 3a shows an array of aligned Sn

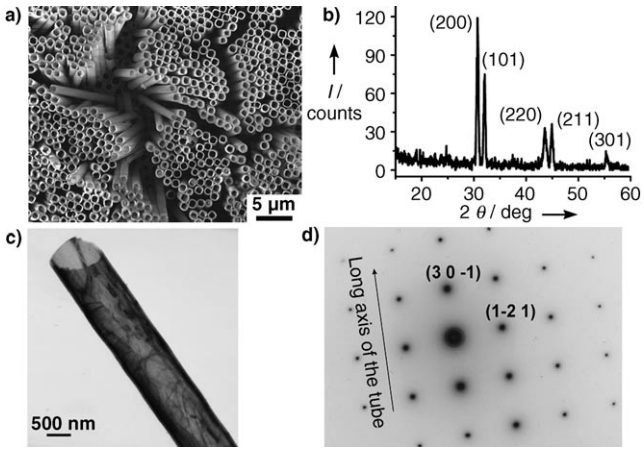

Figure 3. a) SEM image of a laterally extended array of Sn nanotubes with a diameter of 1000 nm, protruding from the macroporous silicon matrix; b) XRD pattern of aligned, partially released tin tubes. All reflections are indexed on the basis of JCPDS card no. 04-673; c) tin nanotube after removal of the silicon template; d) indexed SAED pattern of a single tin nanotube (zone axis [123]), indicating its single-crystalline character.

tubes protruding from a partially removed template. They are uniform in size and have a wall thickness of approximately 150 nm. All reflections in the X-ray diffraction pattern (Figure 3b) can be indexed for tetragonal β-Sn[16] without ambiguity, indicating that the reduction of tin(II) selenide is quantitative. Figure 3c shows an individual tin tube (d = 1000 nm) after removal of the silicon template, and an indexed SAED pattern is depicted in Figure 3d.

When $Sn(SePh)_4$ was infiltrated into porous alumina and annealed at 650 °C a big difference in the oxidizing power of the walls of small pores etched with sulfuric acid and the walls of larger pores etched with phosphoric acid became apparent. Whereas the thicker, less acidic walls of the larger pores did not lead to the oxidation of SnSe, single-crystalline SnO_2 nanowires with a high aspect ratio and diameters of 25 nm were obtained from porous alumina templates etched with sulfuric acid. This is in accordance with the higher defect

concentration, the increased acidity, and the presence of electrolyte anions and residual water in the pore walls of templates etched with sulfuric acid.[12] Figure 4a shows a TEM image of SnO_2 nanowires at low magnification. They typically

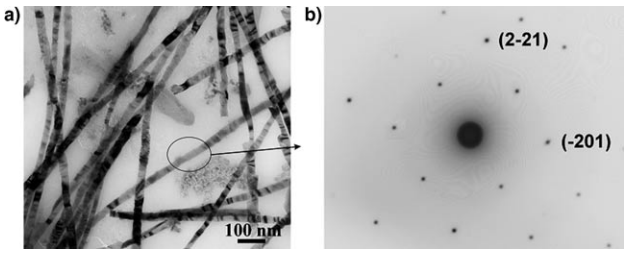

Figure 4. a) TEM image of single-crystalline SnO_2 nanowires with a diameter of 25 nm; b) indexed SAED pattern (zone axis [122]) of the marked section of the SnO_2 nanowire seen in (a).

have aspect ratios (length over diameter) greater than 100. The nonuniform contrast of these nanowires is due to bending contours, thickness fringes, and planar defects.[17] An indexed SAED pattern of part of a section of a single-crystalline SnO_2 nanowire (Figure 4a) is depicted in Figure 4b.

A high-resolution TEM micrograph of a selected area of an individual nanowire of tetragonal SnO_2 (Figure 5) again shows the single-crystalline nature of the wires. The interplanar spacing of $d = 3.34$ Å (Figure 5c) could be assigned to {110} planes of the SnO_2 lattice described in space group $P4_2/mnm$.[18]

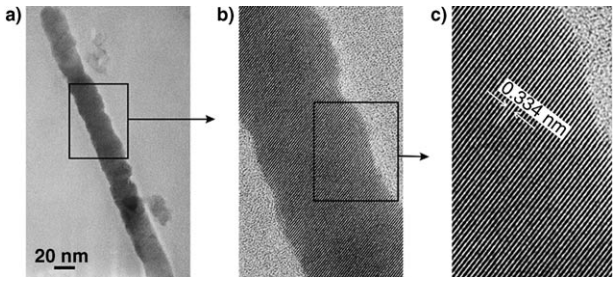

Figure 5. a) Segment of an individual SnO_2 nanowire with a diameter of 25 nm; b) enlarged section of the nanowire, indicating the good homogeneity and crystallinity; c) high-resolution image of a part of (b), showing {110} lattice fringes of SnO_2.

In conclusion, the selective reactivity of the pore walls of porous alumina and macroporous silicon, which leads not just to a surface modification but to a complete conversion of the one-dimensional nano-objects, allows the preparation of monodisperse tubes and nanowires of three different target materials—SnSe, SnO_2, and Sn—from a single-source precursor, $Sn(SePh)_4$. The enhanced reaction temperature for the oxidation within the pores facilitated the formation of single-crystalline nanowires of SnO_2.

Experimental Section

Synthetic procedures: The precursor compound $Sn(SePh)_4$ was synthesized according to a literature procedure.[4]

Sample preparation: The templates were prepared according to procedures described elsewhere.[1,2] For the SnSe and SnO_2 wires, as well as for the Sn tubes shown in Figure 1 and Figures 3–5, the $Sn(SePh)_4$ was melted on the template surface at a temperature of 110 °C. For the SnSe tubes shown in Figure 2, a solution of 5 wt % $Sn(SePh)_4$ in chloroform was applied dropwise onto the template surface. Subsequently, thermolysis was performed at 350 °C, and or alternatively, SnSe was converted into SnO_2 or Sn at 650 °C. All thermolytic reactions and annealing procedures were performed in corundum crucibles under argon. The templates were selectively removed either partially or completely by etching with a 20 wt % aqueous solution of potassium hydroxide at 70 °C. The resulting suspension was washed with deionized water several times until it was neutral.

X-ray diffraction measurements: XRD measurements were performed with a Philips X'pert MRD diffractometer with a $Cu_{K\alpha}$ radiation source, cradle, and secondary monochromator in a $\theta/2\theta$ geometry. The wires and tubes were aligned within the pores of the templates. Their long axes were parallel, and the template surface was perpendicular to the plane defined by the incident beam and the detector.

Electron microscopy: SEM images of both the completely released tubes, which were deposited on conductive substrates (highly doped silicon wafers), and the partially liberated tubes standing in the matrix of the partially etched templates were obtained using a field-emission scanning electron microscope JEOL JSM 6300F at an accelerating voltage of 5 kV. For TEM imaging and electron diffraction recording, aqueous suspensions of the nano- and micro-objects were applied dropwise onto copper grids coated with a holey carbon film. The samples were investigated in a JEM 1010 microscope operated at 100 kV. High-resolution TEM images shown in Figure 5 were recorded with a high-resolution TEM (JEM 4010 operating at 400 kV).

Received: July 29, 2005
Published online: November 30, 2005

Keywords: nanostructures · selenides · template synthesis · tin

[1] a) H. Masuda, K. Fukuda, *Science* **1995**, *268*, 1466; b) H. Masuda, M. Satoh, *Jpn. J. Appl. Phys.* **1996**, *35*, L126; c) H. Masuda, F. Hasegawa, S. Ono, *J. Electrochem. Soc.* **1997**, *144*, L127; d) H. Masuda, K. Yada, A. Osaka, *Jpn. J. Appl. Phys. Part 2* **1998**, *37*, L1340; e) P. Braunstein, H.-P. Kormann, W. Meyer-Zaika, R. Pugin, G. Schmid, *Chem. Eur. J.* **2000**, *6*, 4637; f) K. Nielsch, J. Choi, K. Schwirn, R. B. Wehrspohn, U. Gösele, *Nano Lett.* **2002**, *2*, 677.

[2] a) V. Lehmann, *J. Electrochem. Soc.* **1993**, *140*, 2836; b) A. Birner, U. Grüning, S. Ottow, A. Schneider, F. Müller, V. Lehmann, H. Föll, U. Gösele, *Phys. Status Solidi A* **1998**, *165*, 111.

[3] a) C. R. Martin, *Science* **1994**, *266*, 1961; b) C. A. Huber, T. E. Huber, M. Sadoqi, J. A. Lubin, S. Manalis, C. B. Prater, *Science* **1994**, *263*, 800; c) B. B. Lakshmi, P. K. Dorhout, C. R. Martin, *Chem. Mater.* **1997**, *9*, 857; d) M. Steinhart, J. H. Wendorff, A. Greiner, R. B. Wehrspohn, K. Nielsch, J. Schilling, U. Gösele, *Science* **2002**, *296*, 1997; e) M. Steinhart, Z. Jia, A. Schaper, R. B. Wehrspohn, U. Gösele, J. H. Wendorff, *Adv. Mater.* **2003**, *15*, 706; f) N. I. Kovtyukhova, T. E. Mallouk, T. S. Mayer, *Adv. Mater.* **2003**, *15*, 780; g) M. Steinhart, R. B. Wehrspohn, U. Gösele, J. H. Wendorff, *Angew. Chem.* **2004**, *116*, 1356; *Angew. Chem. Int. Ed.* **2004**, *43*, 1334; h) L. Zhao, M. Steinhart, M. Yosef, S. K. Lee, T. Geppert, E. Pippel, R. Scholz, U. Gösele, S. Schlecht, *Chem. Mater.* **2005**, *17*, 3; i) P. Göring, E. Pippel, H. Hofmeister, R. B. Wehrspohn, M. Steinhart, U. Gösele, *Nano Lett.* **2004**, *4*, 1121.

[4] S. Schlecht, M. Budde, L. Kienle, *Inorg. Chem.* **2002**, *41*, 6001.

[5] M. T. S. Nair, P. K. Nair, *Semicond. Sci. Technol.* **1991**, *6*, 132.
[6] a) A. Bennouna, P. Y. Tessier, M. Priol, Q. Dang Tran, S. Robin, *Phys. Status Solidi B* **1983**, *117*, 51; b) K. Bindu, P. K. Nair, *Semicond. Sci. Technol.* **2004**, *19*, 1348.
[7] T. Subba Rao, B. K. Samanata Ray, A. K. Chaudhuri, *Thin Solid Films* **1988**, *165*, 257.
[8] Y.-G. Gao, J.-S. Hu, H.-M. Zhang, H.-P. Liang, L.-J. Wan, C.-L. Bai, *Adv. Mater.* **2005**, *17*, 746.
[9] J.-G. Wang, M.-L. Tian, T. E. Mallouk, M. H. W. Chan, *Nano Lett.* **2004**, *4*, 1313.
[10] M. L. Tian, J. Wang, J. Snyder, J. Kurtz, Y. Liu, P. Schiffer, T. E. Mallouk, M. H. W. Chan, *Appl. Phys. Lett.* **2003**, *83*, 1620.
[11] a) D.-F. Zhang, D.-L. Sun, J.-L. Yin, C.-H. Yan, *Adv. Mater.* **2003**, *15*, 1022; b) M. Law, H. Kind, B. Messer, F. Kim, P. Yang, *Angew. Chem.* **2002**, *114*, 2511; *Angew. Chem. Int. Ed.* **2002**, *41*, 2405; c) Y. Liu, J. Dong, M. Liu, *Adv. Mater.* **2004**, *16*, 353; d) Z. R. Dai, J. L. Gole, J. D. Sout, Z. L. Wang, *J. Phys. Chem. B* **2002**, *106*, 1274; e) B. Liu, H. C. Zeng, *J. Phys. Chem. B* **2004**, *108*, 5867; f) M. Zheng, G. Li, X. Zhang, S. Huang, Y. Lei, L. Zhang, *Chem. Mater.* **2001**, *13*, 3859.
[12] J. Choi, Y. Luo, R. B. Wehrspohn, R. Hillebrand, J. Schilling, U. Gösele, *J. Appl. Phys.* **2003**, *94*, 4757.
[13] R. Kniep, P. Lamparter, S. Steeb, *Angew. Chem.* **1989**, *101*, 975; *Angew. Chem. Int. Ed. Engl.* **1989**, *28*, 951.
[14] H. G. von Schnering, H. Wiedemeier, *Z. Kristallogr.* **1981**, *156*, 143.
[15] T. Krieg, M. Yosef, S. Schlecht, unpublished results. A 250-mg sample of $Sn(SePh)_4$ was suspended in 50 mL of wet diethylene glycol and heated under reflux for 20 h. The reaction mixture was allowed to cool to room temperature, and the resulting off-white solid was washed filtered, washed with acetone, and air dried. An XRD pattern of the product showed the formation of SnO_2 in $>90\%$ yield with some SnSe present.
[16] β-Sn: JCPDS entry no. 04-673.
[17] Y. Ding, Z. L. Wang, *J. Phys. Chem. B* **2004**, *108*, 12280.
[18] SnO_2: JCPDS entry no. 21-1250.

